The Retreated Tendency of the COVID-19 Pandemic

Zhengkang Zuo (✉ 1801110646@pku.edu.cn)
Peking University https://orcid.org/0000-0003-1255-6332

Research Article

Keywords: COVID-19, Retreated tendency, Potential periodicity, Prediction

Posted Date: July 15th, 2021

DOI: https://doi.org/10.21203/rs.3.rs-704901/v1

ENVIRONMENTAL HEALTH

Article

The Retreated Tendency of the COVID-19 Pandemic

Zhengkang Zuo [1], *

[1] School of Earth and Space Science, Peking University, Beijing, 100871, China; 1801110646@pku.edu.cn;
* Correspondence: 1801110646@pku.edu.cn;

Abstract: The novel virus (COVID-19) pandemic threats the global most since the World War II yet difficult to design effective policy to respond it because widely utilized models only support to predict the future tendency within a narrow time-window. Hereby, we developed a Benchmark, Amendment and Validation model (BAVM) combined with the hypothesis of potential periodicity of COVID-19 to devote jointly the retreated prediction of pandemic within a broad time-window. Results exhibits the 4-month of potential periodicity between two adjacent peaks of pandemic (t=–1.56, p=12.4%). Besides, whether or not the peak emergence has no effect on COVID-19 dynamic trajectory, but the time to firstly peak affects. Meanwhile, uprising the quarantine rate exhibits the earlier expedition towards the first peak emergence (9.7% vs. 6.2%, p=4.1%). On the contrary, the delay of first peak increased the infection rate (0.6% vs. 0.3%, p=1.5%) but also the discharge rate (65% vs. 74%, p=3.8%). Moreover, the indication of the retreated tendency of COVID-19 pandemic is that the next peak should emerge but in fact vanished after one periodicity. Otherwise, the pandemic enters into the next worse phase, typical of high mortality (5% vs. 3.4%, p=5.3%) and low discharge rate (65.8% vs. 74.1%, p=4.2%).

Keywords: COVID-19; Retreated tendency; Potential periodicity; Prediction

1. Introduction

The well-known novel virus (COVID-19) is a new strain of coronavirus family, declared by the World Health Organization (WHO) as a pandemic [1] and an in-depth understanding of COVID-19 dynamics and according drivers is vital to design effective policy responses to mitigate it. Previous studies mainly aim to uncover driving factors such as natural factors and non-natural factors. First, NATURE and SCIENCE published articles affirming the positive effect of non-natural interventions such as lock down on mitigating the pandemic in China [2, 3]. However, Coccia agreed that a longer period of lockdown does not reduce significantly fatality rate and even has a negative impact on economic growth, further declining healthcare investment and causing more deaths, a vicious cycle [4]. Besides, Yechezkel et al also supported that human mobility and poverty are two key drivers of COVID-19 transmission and control, but those two drivers are contradictory to achieve because slowing human mobility during the pandemic is at cost of heavy restrictions (such as lock down), further leading economic crisis and exacerbating poverty [5]. Thus, Wang et al recommended a trade-off strategy between pandemic control and regular social activities through the spatiotemporal heterogeneity to replace the broad sweeping interventions [6, 7]. On top of mentioned contradictory non-natural drivers, we cannot rule out the possibility that the observed COVID-19 dynamic trajectory is partially attribute to other unknown climatic factors [2, 3]. Currently, many previous studies affirmed temperature [8, 9], humidity [10, 11], solar radiation [10, 12], aerosol [13, 14] and wind speed [15, 16] as main potential natural drivers. However, EARTHS FUTURE published an article summarizing 46 diverse and even contradictory conclusions concerning effects of those natural drivers on COVID-19 dynamic trajectory [17]. Notably, one of the significant reasons to cause contradictory determinants of those

drivers aforesaid is that the reported pandemic data are quite sensitive to according quarantine policy made by government, hardly revealing the real COVID-19 dynamic trajectory. Sometimes a sudden increase of morbidity does not necessarily reveal the real infection increase yet an outcome of probably changed quarantine policy, making consequent results suspicious. Owing to this, to reduce the sensitivity of utilized trajectory data to quarantine policy is the first contribution of this work.

On top of uncovering potential drivers of COVID-19, another effort is to predict the dynamic tendency of pandemic trajectory. In previous studies, various susceptible-infected-removed (SIR) models and their extensions are widely used [18-23]. However, PNAS published an article to suspect that these models are not yet capable to anticipate the forthcoming COVID-19 dynamic trajectory even if being good at reproducing empirical data through suitably chosen parameters [24]. The same drawback also existed in machine learning model (China case) [25], and auto-regression integrated moving average (ARIMA) model (Spain case) [26], respectively. Apart from the aforementioned sensitivity of COVID-19 data to quarantine policy, the future trajectory of ongoing pandemic is so sensitive to parameter values of those models that predictions are only meaningful within a narrow time window and in probabilistic terms, much as what we are used to in weather forecasts [24]. Recently, Coccia proposed an index to quantify environmental risk of exposure to future pandemics of the COVID-19, supporting a proactive environmental strategy to help policymakers to prevent future pandemic [27]. However, it is only meaningful when the COVID-19 trajectory entered the retreated phase, because the separation model proposed by Zuo et al exhibited the principal response of COVID-19 trajectory to non-natural factors and subordinate response to environmental factors [17]. Thus, the second contribution of this work is to predict COVID-19 dynamic tendency within a broad time window through the hypothesis of potential periodicity of COVID-19. Consequently, we also expected to predict the retreated indication of this pandemic, which is quite significant for all humans' lives and well-being.

2. Materials and Methods

2.1. Data Collection

Two types of data (either a certain day's data or the time-series data) together support our work. The first data type reveals four COVID-19 pandemic trajectories on August-31, 2020 at 113 countries by the cumulative number of confirmed cases, deaths, discharges and in-ICU cases, respectively (all data are available in WHO reports [28]). Contemporaneously, data of the number of populaces participating the COVID-19 detecting-pool are available at the world info meter of COVID-19 (https://www.worldometers.info/coronavirus/). Onward, the second type of data is the time-series of total confirmed COVID-19 cases from January-21, 2020 to August-31, 2020 available at the COVID-19 data repository (https://github.com/CSSEGISandData/COVID-19), which is utilized to predict the tendency of according trajectories. Besides, Figure 1 shows the geographical locations of 113 investigated countries that made their test size data public. Notably, all original and intermediate data for this work are available in the Zenodo repository (PMC-2021. (2021, June 2). PMC-2021/BAVM-Model: BAVM-Model (Version v1.0.0). Zenodo. http://doi.org/10.5281/zenodo.4892353.)

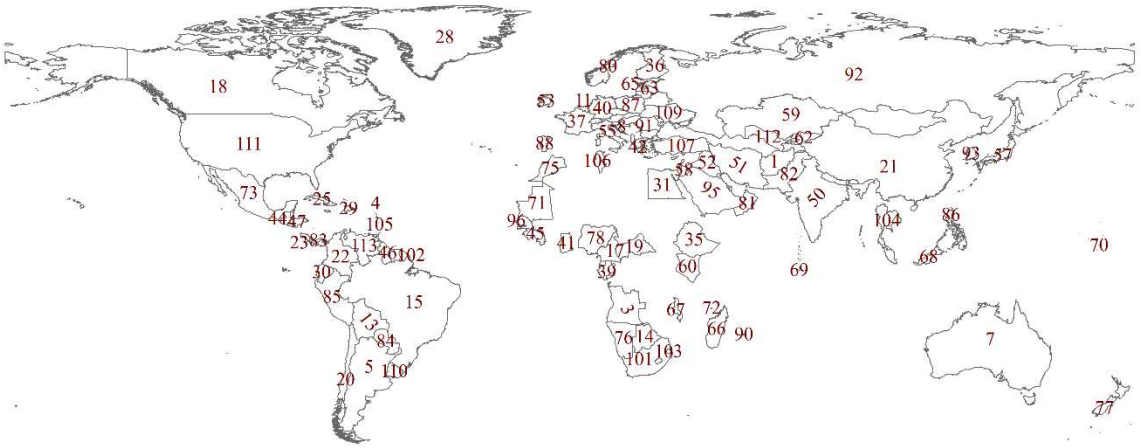

Figure 1. Ggeographical locations of 113 investigated countries. Note that all world maps (Data Source: ArcWorld Supplement) were created using ArcGIS software 10.7.1 by ESRI, which are used herein under license. Copyright ESRI. All rights reserved. For more information about ESRI software, please visit www.esri.com.

2.2. Pandemic Metrics

Derivative pandemic metrics are widely used in many statistical researches concerning distinct COVID-19 pandemic trajectories, i.e., positive rate [29] and infection rate [30] to uncover the infection-specific characteristic of according trajectories. Besides, the case fatality rate [31], mortality rate [32] and closed case fatality rate [33] are proposed for revealing death-specific characteristic; the discharge rate [34], recovery rate [35] and survival case discharge rate [36, 37] for recovery-specific characteristic; in-ICU case rate [37, 38] and clinical deterioration rate [38] for worsening-specific characteristic, respectively. The details about those metrics calculation are listed in Table A1.

2.3. Benchmark, Amendment and Validation Model

Consider the following complex phenomena of COVID-19 pandemic transmission estimated by pandemic metrics. Taking the pandemic metric "positive rate" as an example, we can find (Figure 2) that this metric is sensitive to the detecting rate (p<0.001), which make the positive rate hard to reveal the real infection phenomena, because the fluctuation of this value may be an outcome of a suddenly changed detecting rate instead of real infection increase or decrease. Likewise, the above phenomena also exist in other metrics, such as "infection rate" (R=0.446, p<0.001). Hereby, the contribution of our proposed BAVM model is that it is indeed benefit for making the above complex phenomena clearer.

Taking a simple example to explain the methodology. Assuming there are two regions A and B (Table 1). Besides, the population of region-A and B are both 10, but there are 10 persons to participate the COVID-19 detection in A whereas only two persons to be detected in B. The result of detection is the five positive in region-A and two positive in B.

Table 1. The simple scenario to explain the BAVM model.

Regions	Population	Tests (Samples)	Positive cases	Detecting rate (Tests/Population)	Positive rate (Positive cases/Tests)	Infection rate (Positive cases/Population)
A	10	10	5	100%	50%	50%
B	10	2	2	20%	100%	20%

The complex phenomena in this scenario is that can we say the positive rate of region-B is higher than that of A? Absolutely cannot, because the detecting rate of region-B is only 20%, we cannot convince its 100% of positive rate. On the contrary, the 50% of positive rate of region-A could be convinced to reveal the real infection due to its 100% detecting rate. However, the problem is that how to evaluate the pandemic situation of region-B? Given the negative response of the positive rate to the detecting rate, low

detecting rate corresponds to the risk to overestimate the positive rate. Similarly, given the positive response of the infection rate to the detecting rate, low detecting rate corresponds to the risk to underestimate the infection rate. Thus in region-B, we overestimated its positive rate (100%) and underestimated its infection rate (20%), respectively.

However, the pandemic situation in region-A can be a benchmark for B, and we use the "metric distance" of other regions to the benchmark to estimate its relative data confidence. Indeed, it can also reveal the relative level of risk to overestimate or underestimate the pandemic of different regions. In Table 2, taking the positive rate as an example, the metric distance from region-A to B is 50% ÷ 100% = 0.5. The shorter this distance, the higher risk to overestimate the positive rate of region-B. Besides, taking the infection rate as an example, the metric distance from region-A to B is 50% ÷ 20% = 2.5. The longer this distance, the higher risk to underestimate the infection rate of region-B. To reduce the above risk, we average the metric distance and re-calculated the amended positive rate and infection rate in Table 3.

Table 2. Risk analysis of the positive rate and infection rate

Regions	Positive rate	Infection rate	Metric distance (positive rate)	Metric distance (infection rate)
B	100%	20%	0.5	2.5
Risk to overestimate	√	×	×	√
Risk to underestimate	×	√	√	×

Table 3. Risk analysis of the amended positive rate and infection rate

Regions	Average metric distance	Amended positive rate	Amended infection rate
B	1.5	33.3%	33.3%
Risk to overestimate	×	×	×
Risk to underestimate	×	×	×

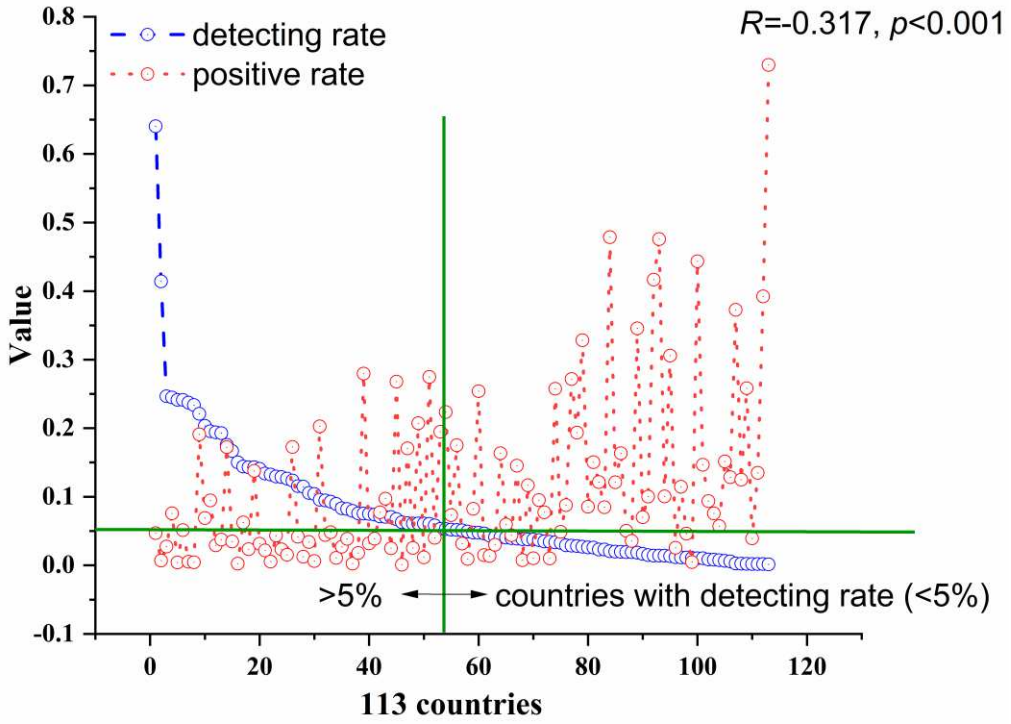

Figure 2. The significantly negative response of one of pandemic metrics "positive rate" to detecting rate (R=-0.317, p<0.001).

Therefore, in general, the BAVM model to compensate the overestimation (↑) / underestimation (↓) risk of existing COVID-19 pandemic trajectory data contains three

steps. The **first step** concerns the benchmark. The *Chi*-square test and *Pearson*-correlation test [44] are jointly utilized to measure the coupling association of four groups of pandemic trajectories (Table 4) with region-wise detecting-strategy of COVID-19 cases (that is testing rate [39]) to output several groups of overvalued and undervalued trajectory data in the case of *p*-value not beyond 0.05. Besides, each mentioned trajectory sequence contains 113 data points reported from investigated countries (Equation 1). Onward, the data confidence of according trajectory points are sequenced by data of testing rate. For instance, trajectory data concerning the first metric (Table A1) reported from Bahrain (testing rate: 64.04%) is 3%, containing higher data confidence than Denmark (0.29%; testing rate: 41.41%). Moreover, trajectory data reported from Bahrain own the highest confidence, being a benchmark ($t_{\uparrow}^{1}$ and $t_{\downarrow}^{1}$) to amend the correlating trajectory data ($t_{\uparrow}^{k}$ and $t_{\downarrow}^{k}$, k>1) reported from the other countries. The **second step** is to amend a group of overvalued and undervalued trajectory data by quotient average model (QAM) (Equation 2). Specifically in Equation 2, two quotients between the benchmark of the overvalued / undervalued trajectory data and the other to-amend trajectories are $q_{\downarrow}^{k}$ (undervalued) and $q_{\uparrow}^{k}$ (overvalued), respectively. Onward, amended trajectory sequences (Equation 3) are obtained through the average quotient ($\tilde{q}^{k}$) of those two quotients. The **third step** is to validate the coupling association between amended trajectories and detecting-strategy of COVID-19 cases by *Chi*-square test and *Pearson*-correlation test yet again. The consequence of *p*-value beyond 0.05 reveals the successful compensation to aforementioned overestimation / underestimation of existing trajectory data.

$$\begin{cases} \boldsymbol{T}_{\uparrow} = \left\{ \overbrace{\tilde{t}_{\uparrow}^{1}}^{\text{Benchmark point}} , \overbrace{t_{\uparrow}^{2}, \ldots, t_{\uparrow}^{n}}^{\text{To-amend trajectory points}} \right\} \\ \boldsymbol{T}_{\downarrow} = \left\{ \overbrace{\tilde{t}_{\downarrow}^{1}}^{\text{Benchmark point}} , \overbrace{t_{\downarrow}^{2}, \ldots, t_{\downarrow}^{n}}^{\text{To-amend trajectory points}} \right\} \end{cases} \quad (1)$$

In Equation 1, $\boldsymbol{T}_{\uparrow}$ and $\boldsymbol{T}_{\downarrow}$ individually represents the overvalued and undervalued trajectory sequence. Moreover, $t_{\uparrow}^{k}$ and $t_{\downarrow}^{k}$ demonstrate two types of specific trajectory points reported from the k^{th} (k>1) country (n=113). Specifically, $t_{\uparrow}^{1}$ and $t_{\downarrow}^{1}$ are both benchmarks to amend the other 112 trajectory points. Onward, Figure 3 combined Equation 2 represent the quotient average model (QAM), where $t_{\uparrow}^{1}$ and $t_{\downarrow}^{1}$ are both benchmarks to amend the other 112 trajectory points $t_{\uparrow}^{k}$ and $t_{\downarrow}^{k}$ (k>1). Besides, $q_{\uparrow}^{k}$ and $q_{\downarrow}^{k}$ are two quotients between benchmarks and the other to-amend trajectory points (k>1). Subsequently, $\tilde{q}^{k}$ is the average outcome of those two quotients, and $\widetilde{t_{\uparrow}^{k}}$ and $\widetilde{t_{\downarrow}^{k}}$ are final amended trajectory points (k>1). In Equation 3, $\widetilde{\boldsymbol{T}}_{\uparrow}$ and $\widetilde{\boldsymbol{T}}_{\downarrow}$ separately represent the final amended trajectory sequence.

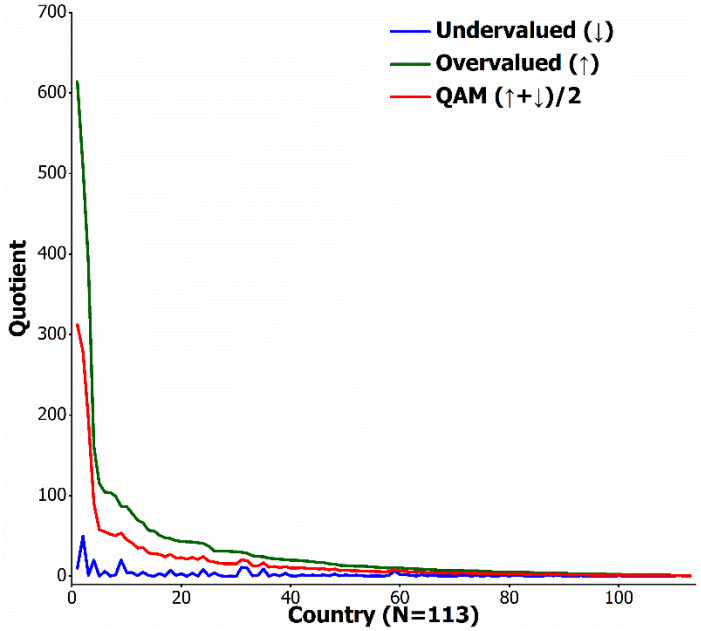

Figure 3. The quotient average model (QAM) to amend trajectories (positive rate and infection rate) with risk of over/under estimation. Specifically, the green line represents the overvalued quotient between benchmark and to-amend trajectory points, whereas the blue line demonstrates the undervalued quotient. Onward, the red line shows the average quotient as the outcome of QAM model to amend the positive rate (Figure 6a) and infection rate (Figure 6c).

$$\begin{cases} \tilde{t}_{\uparrow}^{k} = {t_{\uparrow}^{k}}/{\tilde{q}^{k}}, \tilde{t}_{\downarrow}^{k} = {t_{\downarrow}^{k}}/{\tilde{q}^{k}}, k > 1 \\ \tilde{q}^{k} = {\left(q_{\uparrow}^{k} + q_{\downarrow}^{k}\right)}/{2} \\ q_{\downarrow}^{k} = {t_{\uparrow}^{1}}/{t_{\uparrow}^{k}}, q_{\uparrow}^{k} = {t_{\downarrow}^{1}}/{t_{\downarrow}^{k}} \end{cases} \quad (2)$$

$$\begin{cases} \tilde{\boldsymbol{T}}_{\uparrow} = \left\{ t_{\uparrow}^{1}, \overbrace{\tilde{t}_{\uparrow}^{2}, \ldots, \tilde{t}_{\uparrow}^{n}}^{\text{Amended trajectory points}} \right\} \\ \tilde{\boldsymbol{T}}_{\downarrow} = \left\{ t_{\downarrow}^{1}, \overbrace{\tilde{t}_{\downarrow}^{2}, \ldots, \tilde{t}_{\downarrow}^{n}}^{\text{Amended trajectory points}} \right\} \end{cases} \quad (3)$$

2.4. Hypothesis of Pandemic Periodicity and Retreated Indication

The time interval between two successive peaks of the COVID-19 pandemic trajectory reveals its potential periodicity of according trajectory (Figure 4). In spite of the intricate and coupling interaction between the pandemic trajectory and numerous unknown driving factors [17], the periodicity potentially exists due to the systematic regularity of two main driving factors such as human interventions [2, 3] and climate change [17]. Owing to this, it is capable to predict the **retreat tendency** of this pandemic based on the probability of another round of pandemic peak contained by the probable time interval (Equation 4). Consequently, the afterward peak that rejects to emerge within the expected time interval is the probable vanished peak, an indication of the retreat tendency of the COVID-19 pandemic trajectory across the global or certain regions.

$$P\{\rho = 1 | t_{\rho} \in [t_{k+1} - \Delta t, t_{k+1} + \Delta t]\} \quad (4)$$

In Equation 4, t_{ρ} indicates a predicted time to reach another round of pandemic peak; t_{k+1} signifies a center of a probable time interval, and Δt is a prior estimated threshold.

Onward, ρ = 1 represents an emerged successive peak, otherwise a probable vanished peak (ρ = 0).

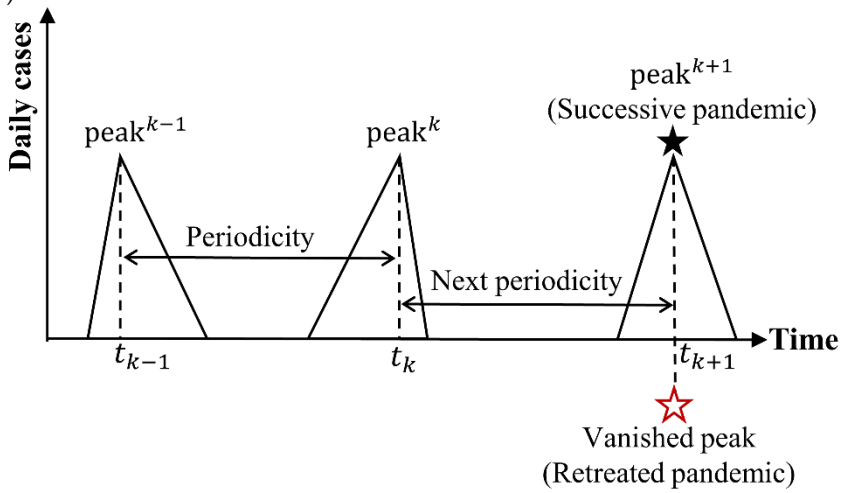

Figure 4. The COVID-19 pandemic periodicity and retreated back indication. Specifically, each trigon represents a pandemic phase, in which each dotted line describes the corresponding peak time. Besides, the time interval between t_{k-1} and t_k describes the observed periodicity. Onward, the time interval between t_k and t_{k+1} predicts the successive theoretic periodicity.

3. Results

3.1. Screen COVID-19 Pandemic Trajectories with Risk to Over/Under Estimation

Table 4 shows the coupling associations of 10 pandemic trajectories with distinct testing rate data reported from 113 countries. It could be observed that the positive rate exhibits a significant negative association with testing rate (p<0.001). On the contrary, the infection rate shows a significant positive association with testing rate (p<0.001). Thus, above two trajectory data contains the risk of overestimation and underestimation due to the average testing rate not beyond 8% up to date (Figure 5). Besides, despite a significant nonlinear association of the case fatality rate (p=0.030) with testing rate, it is difficult to measure the uncertainty of this trajectory and thus cannot support BAVM model. Notably, the discharge rate and survival case discharge rate both exhibit significant *Pearson* associations with testing rate (p=0.200 and p=0.196) yet fail to reach the significance level of 0.05 in the *Chi*-square test (p=0.110 and p=0.110), hereby, the risk to over/under estimation of these two trajectories could be ignored. Besides, such risk of remnant seven trajectories also fail to exhibit the statistical significance. Consequently, the positive rate and infection rate are screened out to amend in the BAVM model (Section 3.2).

Table 4. The correlation between testing rate and four groups of pandemic trajectories ($^{*}p$ < 0.05, $^{**}p$ < 0.01, $^{***}p$ < 0.001), where the number of trajectory points in each trajectory sequence is 113. Notably, detailed descriptions of ten trajectories are in Table A1.

Group	Trajectory	Testing rate	
		***Chi*-square test**	***Pearson*-correlation test**
1	Positive rate	16.37***	-0.317***
	Infection rate	12.11***	0.446***
2	Case fatality rate	4.686*	-0.010
	Mortality rate	0.080	-0.055
	Closed case fatality rate	2.011	-0.029
3	Discharge rate	2.555	0.200*
	Recovery rate	0.435	0.029
	Survival case discharge rate	2.555	0.196*
4	In-ICU case rate	2.555	-0.120
	Clinical deterioration rate	0.080	-0.076

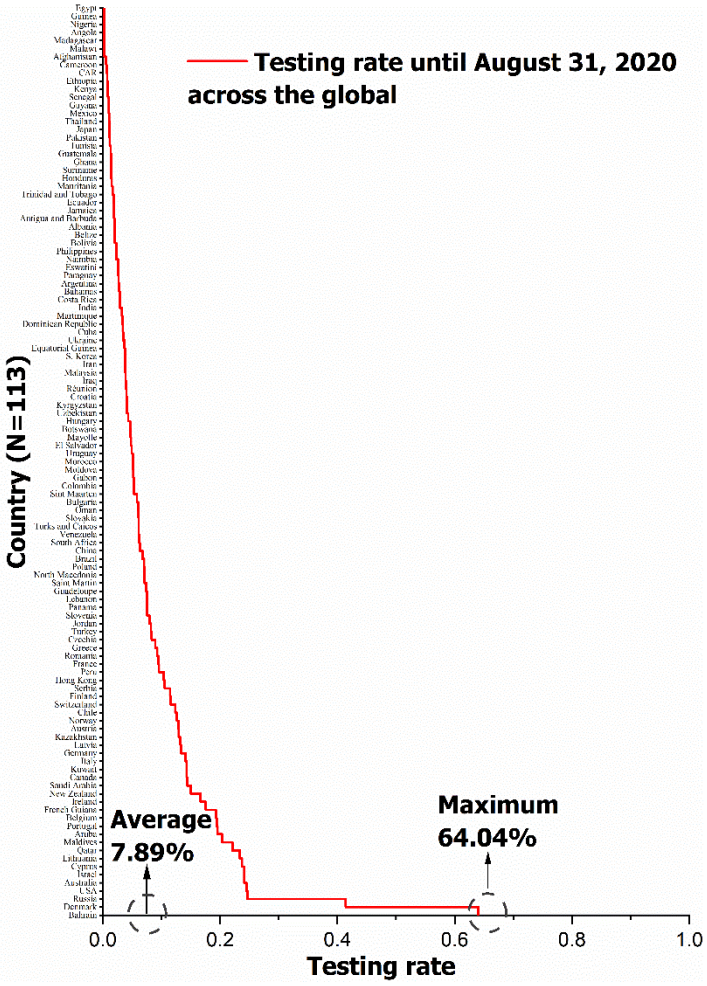

Figure 5. Testing rate reported from 113 investigated countries on August 31, 2020. Specifically, the average and maximum of according data of testing rate is 7.89% and 64.04%, respectively.

3.2. BAVM Model to Reduce Trajectory Risks

Combined Section 3.1 and 2.3, the positive rate reported from Bahrain is a benchmark in BAVM model to amend remnant trajectory points overvalued by the other 112 countries. Similarly, BAVM model also supports to amend remnant-undervalued points in the infection rate sequence. Onward, Figure 6 shows the outcome of BAVM model to overcome two trajectory risks described in Section 3.1. It could be observed that the positive rate with risk of over estimation was recompensed from 11.40% of average data-point down to 1.42% in the case of only 7.89% of average testing rate (Figure 5). Besides, the infection rate with risk of under estimation was compensated from 0.54% of average data-point up to 0.91% in the same case. For example, data-point (73%) in the positive rate (Figure 6a) and data-point (0.1%) in the infection rate (Figure 6c) both reported from Egypt, but that data only owns 0.13% probability to be trusted (Figure 5). However, after the amendment of BAVM model, Egypt exhibits the positive rate down to 0.3% (Figure 6b) and the infection rate up to 0.19% (Figure 6d). Further, Figure 6 also exhibits the similar compensations happened in other countries. Onward, Table 5 shows the outcome of validation in BAVM model that both amended trajectories exhibit insignificant associations with testing rate (χ^2 (113) =0.716 and p=0.398). Thus, the response of amended trajectories to uncertainty risks brought from the current low testing rate (Figure 5) turns to be insensitive.

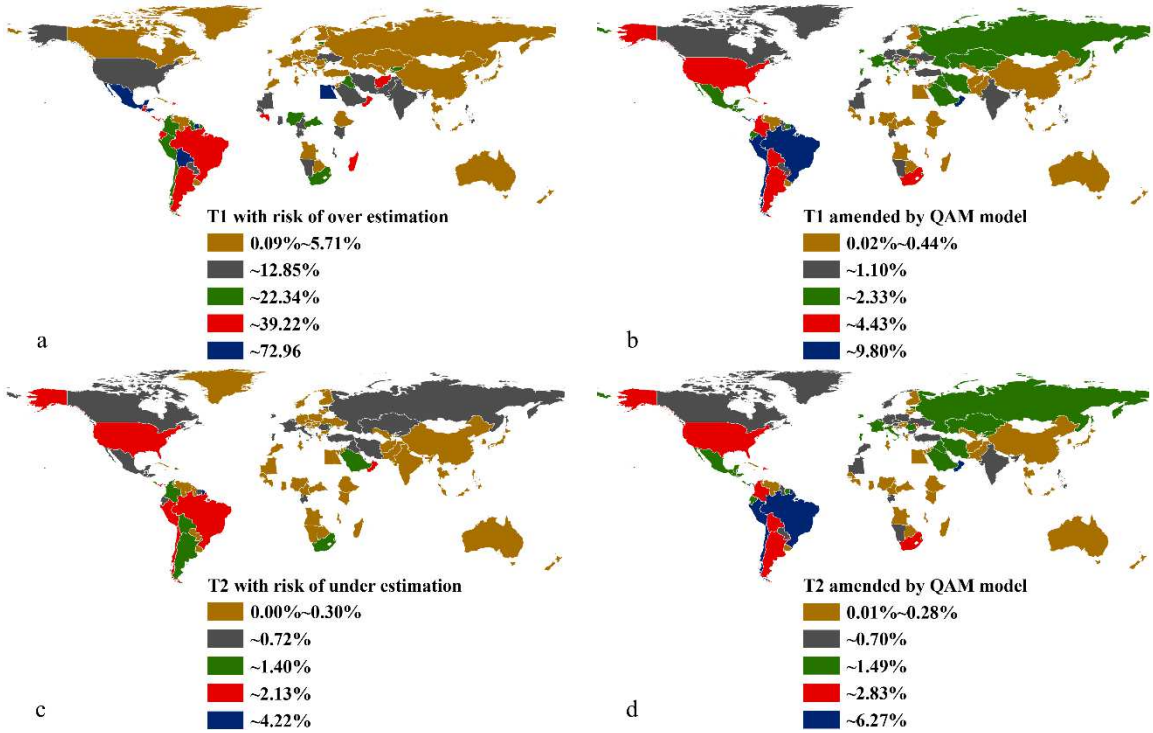

Figure 6. The QAM model to overcome two risks from the positive rate (labeled T1 within figure) and infection rate (labeled T2 within figure). The detailed process of QAM model is in Figure 3. Specifically, Figure 6a and 6c exhibit the spatial distributions of two trajectories (T1 and T2), respectively. Onward, Figure 6b and 6d show final amended two trajectories in BAVM model. Note that all world maps (Data Source: ArcWorld Supplement) were created using ArcGIS software 10.7.1 by ESRI, which are used herein under license. Copyright ESRI. All rights reserved. For more information about ESRI software, please visit www.esri.com.

Table 5. The validation of two amended trajectories in BAVM model ($^{*}p < 0.05$, $^{**}p < 0.01$, $^{***}p < 0.001$). Notably, detailed descriptions of those two trajectories are in Table A1.

	Median	**Trajectory**	**Median**		**χ^2**	***p*-value**
Testing rate		T-1	<0.77% (N=61)	≥0.77% (N=56)	0.716	0.398
	<0.05		31 (50.8%)	26 (46.4%)		
	≥0.05		30 (49.2%)	30 (53.6%)		
		T-2	<0.49% (N=61)	≥0.49% (N=56)	0.716	0.398
	<0.05		31 (50.8%)	26 (46.4%)		
	≥0.05		30 (49.2%)	30 (53.6%)		

3.3. Potential Periodicity of COVID-19 Pandemic

Figure 7a shows that until August 31, 2020, the time-interval between the twice COVID-19 peaks was mainly concentrated in a 4-months period, so the average time-interval was hypothesized as a 4-months period. On top of that, the time-interval (Figure 7b) in 52% of countries (N=32), 19% of countries (N=12), 23% of countries (N=14) and 6% of countries (N=4) showed a 4-months, 5-months, 3-months and 2-months period, respectively. Therefore, the alternative hypothesis (Table 6) in *One*-sample *t*-test was accepted (t (62) =-1.56, p=0.124) and the average time-interval ($\bar{X}$=3.84) between the twice peaks in sampled countries was statistically equal to the hypothesized population mean (u_0=4). In this regard, the initially hypothesis about the potential periodicity—despite of not knowing the existence of periodicity—of COVID-19 pandemic was made as a 4-months period.

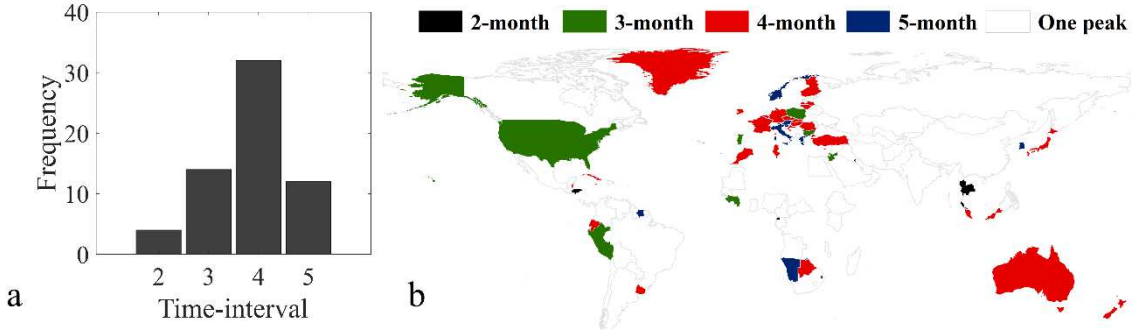

Figure 7. The time-interval between twice-pandemic peaks from 62 countries where the pandemic recurred. Onward, Figure 7a exhibits the frequency distribution histogram with according value of 4, 14, 32 and 12, respectively. Besides, Figure 7b exhibits spatial distribution of those countries. Specifically, black-shaded patch represents 2-month time-interval between twice peaks, green-shaded patch (3-month), red-shaded patch (4-month), and blue-shaded patch (5-month). Note that all world maps (Data Source: ArcWorld Supplement) were created using ArcGIS software 10.7.1 by ESRI, which are used herein under license. Copyright ESRI. All rights reserved. For more information about ESRI software, please visit www.esri.com.

Table 6. Result of *One*-sample *t*-test [45] ($^{*}p < 0.05$, $^{**}p < 0.01$, $^{***}p < 0.001$)

	N	Mean	SD	Test-value = 4		
				t	DF	*p*-value
Time-interval	62	3.84	0.81	-1.56	61	0.124

4. Discussion

4.1. Distinction of Peak Wise Trajectories across the Global

Combined with Section 3.2, the amended positive rate and infection rate (Table 7) replaced two trajectories with risk of over/under estimation through BAVM model. Furthermore, this section aims to measure whether or not the emergence of peak will significantly affect investigated pandemic trajectories. Figure 8a shows that until August 31, 2020 the pandemic peak in 83% of countries (N=94; blue-patch) was emerged, but 17% of countries (N=19, red-patch) experienced emergence of no peak. Onward, it was observed that the alternative hypothesis (Table 7) in the *Independent*-sample *t*-test was rejected for testing rate (t (113) =5.41, p<0.01), but was accepted for other ten trajectories. Owing to this, the emergence of peak has no significant effect on trajectories, but testing rate exhibits a significant influence on the emergence of peak. Moreover, peaked trajectory exhibits higher testing rate (Mean = 0.088; SD = 0.096) than trajectory without peak (Mean = 0.030; SD = 0.019). Therefore, expanding the proportion of the populaces in COVID-19 detecting-pool helps the regional/global peak emerge.

Given the 4-month period of potential periodicity of COVID-19 pandemic from January to August (Section 3.3), the month of April splits investigated countries (N=113) into group-1 (peaks in 59 countries emerged **before April**) and group-2 (peaks in 54 countries emerged **after April**) (Figure 8b). The aim is to measure whether the investigated trajectories have significant responses to according time to peak. Table 7 exhibits that the amended positive rate and infection rate both contain significant responses to peaked time (t (113) = 2.49, p = 0.015; t (113) = 2.10, p = 0.038). In addition to the amended positive rate, the amended infection rate with earlier time to peak (before April) exhibit a lower data-point (Mean=0.005; SD=0.008) than that with later time to peak (Mean = 0.011; SD = 0.014). Thus, moving the time to peak ahead is vital for curbing the pandemic. On top of that, uprising the testing rate significantly advances the time to peak (t (113) = -2.07; p= 0.041). Consequently, we suggested the strategy of mass scale testing as a foremost option to fight against the COVID-19 across the global, but if some countries were not capable to support that strategy, the community testing [42] like in China was also an effective strategy to curb this pandemic. Notably, the delay of peaks caused

significantly higher data-point in the discharge rate (Mean = 0.737; SD = 0.194) than the early peaks (Mean = 0.650; SD = 0.241). The reason is that the early peaks will burden the hospitals but the delay of peaks probably made human response gradually effective to curb the pandemic transmission and more deaths [17].

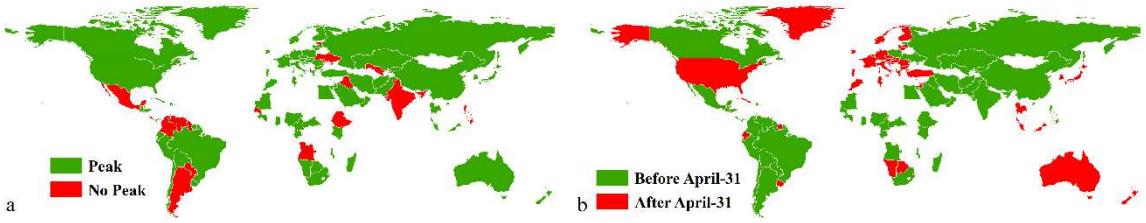

Figure 8. The spatial distribution of two peak wise trajectories. In Figure 8a, pandemic peaks emerged in green-shaded patches, and red-shaded patches represent no peak emerged in those countries. Besides, in Figure 8b, countries with the first pandemic peak emerging before April-31 shaded by green, otherwise, shaded by red. Note that all world maps (Data Source: ArcWorld Supplement) were created using ArcGIS software 10.7.1 by ESRI, which are used herein under license. Copyright ESRI. All rights reserved. For more information about ESRI software, please visit www.esri.com.

Table 7. Distinction of peak wise trajectories through the *Independent*-sample *t*-test [45] ($^{*}p < 0.05$, $^{**}p < 0.01$, $^{***}p < 0.001$). Notably, detailed descriptions of ten trajectories are in Table A1.

Trajectory	Peak	N	Mean	SD	*t*-test		April	N	Mean	SD	*t*-test	
					t	*p*					*t*	*p*
Testing rate	yes	94	0.088	0.096	5.41***	0.000	after	59	0.062	0.096	-2.07*	0.041
	no	19	0.030	0.019			before	54	0.097	0.081		
Amended positive rate	yes	94	0.014	0.019	1.03	0.308	after	59	0.006	0.009	2.49*	0.015
	no	19	0.011	0.010			before	54	0.003	0.005		
Amended infection rate	yes	94	0.009	0.012	0.85	0.395	after	59	0.011	0.014	2.96***	0.004
	no	19	0.006	0.008			before	54	0.005	0.008		
Case fatality rate	yes	94	0.027	0.024	0.19	0.850	after	59	0.024	0.018	-1.40	0.166
	no	19	0.026	0.022			before	54	0.031	0.028		
Mortality rate	yes	94	0.031	0.026	-0.13	0.899	after	59	0.027	0.020	-1.80	0.075
	no	19	0.032	0.025			before	54	0.036	0.030		
Closed case fatality rate	yes	94	0.043	0.050	0.28	0.782	after	59	0.035	0.028	-1.90	0.061
	no	19	0.040	0.028			before	54	0.052	0.060		
Discharge rate	yes	94	0.712	0.227	1.76	0.081	after	59	0.737	0.194	2.10*	0.038
	no	19	0.615	0.172			before	54	0.650	0.241		
Recovery rate	yes	94	0.957	0.050	-0.28	0.782	after	59	0.965	0.028	1.90	0.061
	no	19	0.960	0.028			before	54	0.948	0.060		
Survival case discharge rate	yes	94	0.732	0.233	1.77	0.079	after	59	0.755	0.197	1.97	0.051
	no	19	0.632	0.177			before	54	0.671	0.249		
In-ICU case rate	yes	94	0.002	0.007	-1.03	0.304	after	59	0.002	0.004	-0.93	0.354
	no	19	0.004	0.006			before	54	0.003	0.009		
Clinical deterioration rate	yes	94	0.021	0.055	0.42	0.672	after	59	0.026	0.067	1.06	0.291
	no	19	0.016	0.015			before	54	0.016	0.020		

4.2. Distinction of Peak Wise Trajectories across the Global

Compared to historical pandemics, such as two-phased respiratory virus epidemic in Russia (1889-1892) [40], and three-phased Spanish flu pandemic (1918-1920) [41], the COVID-19 emerged with two phases until August 31, 2020 but still not shrank globally. Combined the method in Section 4.1, this section aims to measure whether or not the varied phases of COVID-19 pandemic will significantly affect according trajectories. Figure 9 exhibits the second-phase of pandemic happened in 55% of countries (N=62; red-patch) yet 45% of countries (N=51, blue-patch) yet to experience the phase-2. Besides, Table 8 exhibits the testing rate in phase-2 (Mean = 0.094; SD = 0.079) is significantly higher than phase-1 (Mean = 0.060; SD = 0.100), revealing the global expansion of according testing rate in second pandemic phase. Notably, the closed case fatality rate in phase-2 (Mean = 0.050; SD = 0.059) exhibits higher value than phase-1 (Mean = 0.034; SD = 0.024). Similarly, the discharge rate, recovery rate and survival case discharge raye in phase-2 all

exhibit lower value than phase-1 (Table 8). Owing to this, the COVID-19 pandemic is expanding in phase-2, which differs from the conclusion drawn by Coccia [43]. There are mainly three reasons for the divergence. First, previous work exhibited a case study in Italy but our work carried out in 113 countries (global-level). Second, only three trajectories concerning incidence, numbers of ICU cases and deaths utilized in previous work, whereas ten trajectories (Table A1) employed in our work. Third, the span of time series data in previous work is from February 2020 to February 2021, but our work spanned from January 2020 to August 2020. In this regard, lessons learned from one case study probably lacks generalization to copy policies to other countries.

Table 8. Distinction of phase wise trajectories through the *Independent*-sample *t*-test [45] ($^{*}p < 0.05$, $^{**}p < 0.01$, $^{***}p < 0.001$). Notably, detailed descriptions of ten trajectories are in Table A1.

Trajectory	Pandemic phase	N	Mean	SD	*t*-test	
					t	*p*
Testing rate	Phase-1	51	0.060	0.100	-2.04*	0.044
	Phase-2	62	0.094	0.079		
Amended T-1	Phase-1	51	0.017	0.022	1.63	0.107
	Phase-2	62	0.011	0.014		
Amended T-2	Phase-1	51	0.011	0.014	1.90	0.061
	Phase-2	62	0.007	0.009		
T-3	Phase-1	51	0.025	0.019	-0.88	0.382
	Phase-2	62	0.029	0.027		
T-4	Phase-1	51	0.028	0.021	-1.27	0.209
	Phase-2	62	0.034	0.029		
T-5	Phase-1	51	0.034	0.024	-1.96	0.053
	Phase-2	62	0.050	0.059		
T-6	Phase-1	51	0.741	0.188	2.06*	0.042
	Phase-2	62	0.658	0.240		
T-7	Phase-1	51	0.966	0.024	1.96	0.053
	Phase-2	62	0.950	0.059		
T-8	Phase-1	51	0.760	0.192	1.99*	0.049
	Phase-2	62	0.678	0.247		
T-9	Phase-1	51	0.002	0.005	-0.40	0.688
	Phase-2	62	0.003	0.009		
T-10	Phase-1	51	0.029	0.071	1.51	0.134
	Phase-2	62	0.014	0.019		

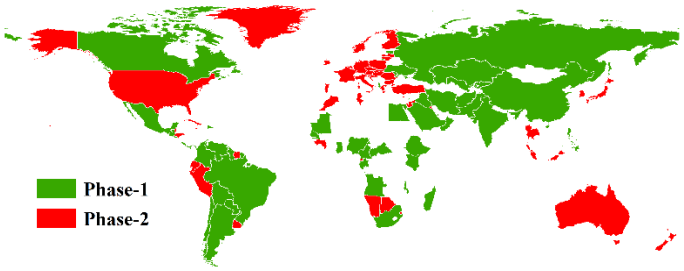

Figure 9. The spatial distribution of the wave (phase) wise trajectory. Specifically, countries (N=51) shaded by green struggled in the first phase of the COVID-19 pandemic until August 31, 2020. Otherwise, countries (N=62) in the second phase shaded by red. Note that all world maps (Data Source: ArcWorld Supplement) were created using ArcGIS software 10.7.1 by ESRI, which are used herein under license. Copyright ESRI. All rights reserved. For more information about ESRI software, please visit www.esri.com.

4.3. Prediction of Global Pandemic Retreated Tendency

Combined Section 4.1 with 4.2, the emergence of successive peak(s) probably brings the severe plight than the former one leading to a worse tendency (blue patches in Figure 11b). Otherwise, combined the hypothesis in Section 2.4, there are strong possibility not

to occur any further peak(s) resulting in a better tendency (red patches in Figure 11b), an indication of retreated tendency in pandemic. In contrast, the pandemic with no emerged peak(s) outcomes a runaway tendency (green patches in Figure 11b). Besides, Figure 11a exhibits the spatial distribution of turning point month (TPM) from January (labeled as 1) to July (labeled as 7), revealing the month-basis emergence of peak, respectively. However, red patches labeled as "8" represent no emergence of peak(s), and brown patches labeled as Recur denote at least twice peaks emerging in those countries.

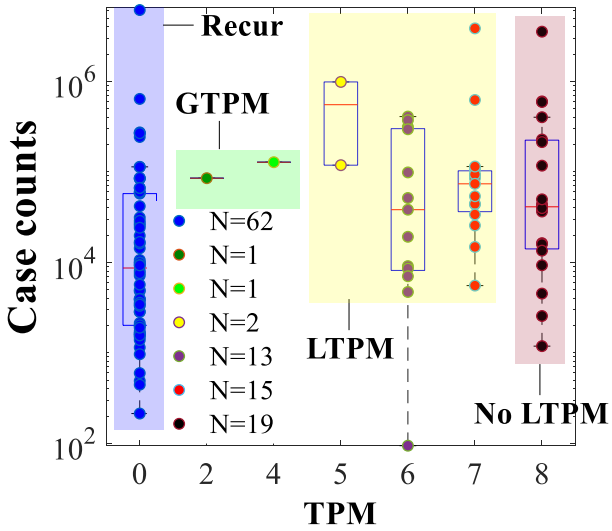

Figure 10. TPM category. Notably, TPM indicates only once peak emerging in according month. Once the pandemic peaks twice, TPM with the first peak turns to TPM-Recur (blue point). **(b)** The four categorized clusters of TPM in 113 investigated countries, such as GTPM, LTPM, No-LTPM and LTPM-Recur. Specifically, **GTPM** (bottle green and pale-green points) reveals that the pandemic peaked only once during two periodicities. Besides, **LTPM** (yellow, pale-brown and orange points) reveals that the pandemic peaked only once during one periodicity. Onward, **LTPM-Recur** (blue points) reveals that the pandemic peaked at least twice during two periodicities. However, **No-LTPM** (nigger-brown points) reveals that the peak(s) did not emerge once during two periodicities.

Furthermore, Figure 11b categorizes the TPM distribution in Figure 11a into the global and the local level that is the global TPM (GTPM) and the local TPM (LTPM). Once the peak emerged, it was the LTPM. In addition, due to the potential periodicity of a 4-months period (Section 3.3), the GTPM emerged based on the hypothesis that the next peak should emerge yet in fact vanished after one periodicity. Thus, the GTPM is the significant month to expect to end this pandemic. Besides, Figure 10 classifies all investigated countries into four clusters that is GTPM, LTPM, LTPM-recur and No-LTPM. Specifically, LTPM-recur happened in 55% of countries (N=62) such as USA, Italy and Peru, whereas GTPM happened in two countries (China and Canada). In addition, LTPM appeared in 27% of countries (N=30) such as Russia and Qatar (TPM=5), Iran and Pakistan (TPM=6), Brazil and South Africa (TPM=7), etc. Unfortunately, No-LTPM emerged in 17% of countries (N=19) such as India and Mexico (TPM=8).

Compared with GTPM that peaked only once during two periodicities, LTPM peaked only once during one periodicity but failed to vanish during the second periodicity. However, LTPM-recur peaked twice during two periodicities yet it may—or may not—peak again after the next periodicity. Moreover, LTPM probably turns to LTPM-recur or GTPM, while LTPM-recur is also possible to shift as GTPM. Owing to this, Figure 11b predicts the global pandemic retreated tendency with three types of TPM.

Consequently, 2%, 67% and 17% countries exhibit a retreated (red-patches), a worse (blue-patches) and a runaway tendency (green-patches) of the pandemic, respectively. Thus, the predicted potential peak(s) would emerge at the months of December 2020, April and August 2021, respectively.

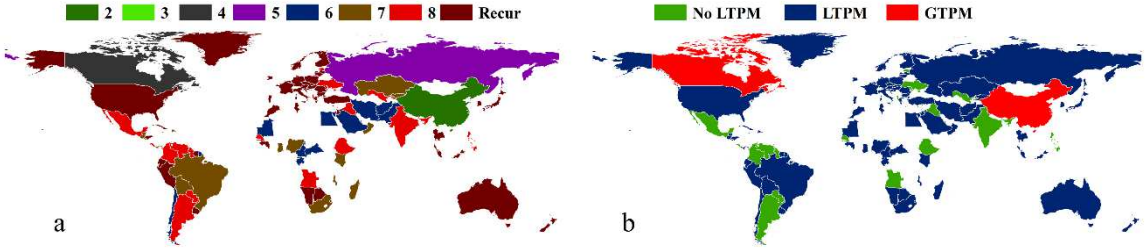

Figure 11. The prediction of global pandemic retreated tendency. In Figure 11a, various colors represent the month to peak for the first time (TPM), revealing the sequence of month-level peaked-time. Notably, the color labeled Recur represents at least twice peaks emerged. Besides, Figure 11b exhibits three types of pandemic tendency. The red/blue/green-shaded patches indicate the better tendency, the worse tendency and the runaway tendency, respectively. Note that all world maps (Data Source: ArcWorld Supplement) were created using ArcGIS software 10.7.1 by ESRI, which are used herein under license. Copyright ESRI. All rights reserved. For more information about ESRI software, please visit www.esri.com.

5. Conclusions

There are two main contributions in this work. First, the proposed BAVM model reduces the sensitivity of COVID-19 dynamic trajectory to the quarantine policy to overcome the drawback in most studies that sometimes a sudden increase of morbidity does not necessarily reveal the real infection increase yet an outcome of probably changed quarantine policy. Such data utilized in relevant studies probably distorted consequent conclusions.

The second contribution aims to predict the COVID-19 dynamic tendency within a broad time window through the hypothesis of potential periodicity of COVID-19, overcoming the drawback of previous studies only supporting the prediction within a narrow time window. Besides, the work also supports to predict the retreated indication of this pandemic, which is quite significant for all humans' lives and well-being. Consequently, several important findings are as summarized.

(1) The potential periodicity of the COVID-19 pandemic peak is around 4-month period (t=-1.56, p=0.124).

(2) Whether or not the peak emergence has no significant effect on COVID-19 dynamic trajectory, but the time to firstly peak significantly affects.

(3) Uprising the quarantine rate significantly advances the time to firstly peak (0.097 *vs* 0.062, p=0.041).

(4) Delay of first peak significantly increased the infection rate (0.006 *vs* 0.003, p=0.015) but also the discharge rate (0.650 *vs* 0.737, p=0.038).

(5) The quarantine rate increased across the global during the second phase of COVID-19 pandemic (0.094 *vs* 0.060, p=0.044).

(6) The COVID-19 global pandemic is expanding in the second phase.

(7) The indication of the retreated tendency of COVID-19 pandemic is that the next peak should emerge yet in fact vanished after one periodicity.

(8) The predicted potential peak(s) would emerge at the months of December 2020, April and August 2021, respectively.

However, the study also has two limitations. First, *Paired*-samples t-test is more reasonable than *Independent*-samples t-test to measure the impact of first and second wave of the COVID-19 pandemic in Section 4.2. Yet, we had no access to obtain complete data reported in the second wave of pandemic within our research time span (2020-1 to 2020-8) to support *Paired*-samples t-test. Hereby, data with longer time span will support our future work. Second, the global-level study combined with more case studies in typical

countries are quite significant to generalize measures aforesaid to support effective policy responses to mitigate the COVID-19 pandemic.

Author Contributions: Single author, Zhengkang Zuo.

Funding: National Key Research and Development Program of China, grant number 2017YFB0503003, funded this research.

Data Availability Statement: All original and intermediate data for this work are available in the Zenodo repository (PMC-2021. (2021, June 2). PMC-2021/BAVM-Model: BAVM-Model (Version v1.0.0). Zenodo. http://doi.org/10.5281/zenodo.4892353.)

Acknowledgments: The authors are indebted to Rui Yao (Wuhan University) and Zengliang Luo (Peking University) for their useful comments and suggestions in the completion of this manuscript.

Conflicts of Interest: The authors declare no conflict of interest.

Appendix A

Table A1. The calculation of 10 derivative pandemic metrics from the raw data, where **N**(·) represents the number of corresponding input contents.

No.	Derivative pandemic metrics	Equations
T-1	Positive rate	N(confirmed cases)/N(tests)
T-2	Infection rate	N(confirmed cases)/N(Population)
T-3	Case fatality rate	N(deaths)/N(confirmed cases)
T-4	Mortality rate	N(deaths)/N(cases | 14 days ago)
T-5	Closed case fatality rate	N(deaths)/[N(deaths) + N(recoveries)]
T-6	Discharge rate	N(recoveries)/N(confirmed cases)
T-7	Recovery rate	N(recoveries)/[N(deaths) + N(recoveries)]
T-8	Survival case discharge rate	N(recoveries)/[N(confirmed cases) − N(deaths)]
T-9	In-ICU case rate	N(critical cases)/[N(confirmed cases) − N(deaths)]
T-10	Clinical deterioration rate	N(critical cases)/[N(confirmed cases) − N(deaths) − N(recoveries)]

References

1. Oud, M.A.A.; Ali, A.; Alrabaiah, H., Ullah, S.; Khan, M.A.; Islam, S. A fractional order mathematical model for COVID-19 dynamics with quarantine, isolation, and environmental viral load. *Advances in Difference Equations* **2021**, *1*, 1-19. https://doi.org/10.1186/s13662-021-03265-4.
2. Lai, S.; et al. Effect of non-pharmaceutical interventions to contain COVID-19 in China. *Nature* **2020**, *585*, 410-413. https://doi.org/10.1038/s41586-020-2293-x.
3. Li, R.; Pei, S.; Chen, B.; Song, Y.; Zhang, T.; Yang, W.; Shaman, J. Substantial undocumented infection facilitates the rapid dissemination of novel coronavirus (SARS-CoV-2). *Science* **2020**, *368*, 489-493. https://doi.org/10.1126/science.abb3221.
4. Coccia, M. The relation between length of lockdown, numbers of infected people and deaths of Covid-19, and economic growth of countries: Lessons learned to cope with future pandemics similar to Covid-19 and to constrain the deterioration of economic system. *Science of The Total Environment* **2021**, *775*, 145801. https://doi.org/10.1016/j.scitotenv.2021.145801.
5. Yechezkel, M.; Weiss, A.; Rejwan, I.; Shahmoon, E.; Ben-Gal, S.; Yamin, D. Human mobility and poverty as key drivers of COVID-19 transmission and control. *BMC public health* **2021**, 21, 1-13. https://doi.org/10.1186/s12889-021-10561-x.
6. Wang, H.; Ghosh, A.; Ding, J.; Sarkar, R.; Gao, J. Heterogeneous interventions reduce the spread of COVID-19 in simulations on real mobility data. *Scientific reports* **2021**, 11, 1-12. https://doi.org/10.1038/s41598-021-87034-z.
7. Wang, L.; Xu, C.; Wang, J.; Qiao, J.; Yan, M.; Zhu, Q. Spatiotemporal heterogeneity and its determinants of COVID-19 transmission in typical labor export provinces of China. *BMC infectious diseases* **2021**, 21, 1-12. https://doi.org/10.1186/s12879-021-05926-x.
8. Wang, J.; Tang, K.; Feng, K.; Lv, W. High temperature and high humidity reduce the transmission of COVID-19. *Available at SSRN 3551767*. doi:10.2139/ssrn.3551767.
9. Zhu, Y. J.; Xie, J. G. Association between ambient temperature and COVID-19 infection in 122 cities from China. *Science of The Total Environment* **2020**, 138201. doi:10.1016/j.scitotenv.2020.138201.

10. Ahmadi, M.; et al. Investigation of effective climatology parameters on COVID-19 outbreak in Iran. *Science of The Total Environment* **2020**, 138705. doi: 10.1016/j.scitotenv.2020.138705.
11. Luo, W.; et al. The role of absolute humidity on transmission rates of the COVID-19 outbreak. *Harvard Library* **2020**. https://doi.org/10.1101/2020.02.12.20022467 or http://nrs.harvard.edu/urn-3:HUL.InstRepos:42639515.
12. Yao, Y.; et al. No Association of COVID-19 transmission with temperature or UV radiation in Chinese cities. *European Respiratory Journal* **2020**. doi:10.1183/13993003.00517-2020.
13. Liu, Y.; Ning, Z.; Chen, Y.; et al. Aerodynamic analysis of SARS-CoV-2 in two Wuhan hospitals. *Nature* **2020**. doi:10.1038/s41586-020-2271-3.
14. Sima, A.; et al. The coronavirus pandemic and aerosols: Does COVID-19 transmit via expiratory particles?, *Aerosol Science and Technology* **2020**, 54, 635-638. doi:10.1080/02786826.2020.1749229.
15. Islam, N.; Shabnam, S.; Erzurumluoglu, A. Temperature, humidity, and wind speed are associated with lower Covid-19 incidence. *medRxiv* **2020**. doi:10.1101/2020.03.27.20045658.
16. Oliveiros, B.; et al. Role of temperature and humidity in the modulation of the doubling time of COVID-19 cases. *medRxiv* **2020**. doi:10.1101/2020.03.05.20031872.
17. Zuo, Z.; Ullah, S.; Yan, L.; Sun, Y.; Peng, F.; Jiang, K.; Zhao, H. Trajectory Simulation and Prediction of COVID-19 via Compound Natural Factor (CNF) Model in EDBF Algorithm. *Earth's Future* **2021**, 9, e2020EF001936. https://doi.org/10.1029/2020EF001936.
18. Abdy, M.; Side, S.; Annas, S.; Nur, W.; Sanusi, W. An SIR epidemic model for COVID-19 spread with fuzzy parameter: the case of Indonesia. *Advances in difference equations* **2021**, 1, 1-17. https://doi.org/10.1186/s13662-021-03263-6.
19. Cooper, I.; Mondal, A.; Antonopoulos, C. G. A SIR model assumption for the spread of COVID-19 in different communities. *Chaos, Solitons & Fractals* **2020**, 139, 110057. https://doi.org/10.1016/j.chaos.2020.110057.
20. Ivorra, B.; Ferrández, M. R.; Vela-Pérez, M.; Ramos, A. M. Mathematical modeling of the spread of the coronavirus disease 2019 (COVID-19) taking into account the undetected infections. The case of China. *Communications in nonlinear science and numerical simulation* **2020**, 105303. https://doi.org/10.1016/j.cnsns.2020.105303.
21. Mohammad, M.; Trounev, A.; Cattani, C. The dynamics of COVID-19 in the UAE based on fractional derivative modeling using Riesz wavelets simulation. *Advances in Difference Equations* **2021**, 1, 1-14. https://doi.org/10.1186/s13662-021-03262-7.
22. Wijaya, K. P.; Ganegoda, N.; Jayathunga, Y.; Götz, T.; Schäfer, M.; Heidrich, P. An epidemic model integrating direct and fomite transmission as well as household structure applied to COVID-19. *Journal of Mathematics in Industry* **2021**, 11, 1-26. https://doi.org/10.1186/s13362-020-00097-x.
23. Zhao, S.; et al. Inferencing super spreading potential using zero-truncated negative binomial model: exemplification with COVID-19. *BMC Medical Research Methodology* **2021**, 21, 1-8. https://doi.org/10.1186/s12874-021-01225-w.
24. Castro, M.; Ares, S.; Cuesta, J. A.; Manrubia, S. The turning point and end of an expanding epidemic cannot be precisely forecast. *Proceedings of the National Academy of Sciences (PNAS)* **2020**. https://doi.org/10.1073/pnas.2007868117.
25. Yang, Z.; et al. Modified SEIR and AI prediction of the epidemics trend of COVID-19 in China under public health interventions. *Journal of Thoracic Disease* **2020**, 12, 165. https://doi.org/10.21037/jtd.2020.02.64.
26. Ceylan, Z. Estimation of COVID-19 prevalence in Italy, Spain, and France. *Science of The Total Environment* **2020**, *729*, 138817. https://doi.org/10.1016/j.scitotenv.2020.138817.
27. Coccia, M. An index to quantify environmental risk of exposure to future epidemics of the COVID-19 and similar viral agents: Theory and Practice. *Environmental research* **2020**, 191, 110155. https://doi.org/10.1016/j.envres.2020.110155.
28. World Health Organization. WHO Coronavirus disease [COVID-2019] situation reports, 17 August 2020. https://www.who.int/docs/default-source/coronaviruse/situation-reports/20200817-weekly-epi-update-1.pdf?sfvrsn=b6d49a76_4.
29. Cordes, J.; Castro, M.C. Spatial analysis of COVID-19 clusters and contextual factors in New York City. *Spatial and Spatio-temporal Epidemiology* **2020**, 34, 100355. https://doi.org/10.1016/j.sste.2020.100355.
30. Morrison, C.N.; Rundle, A.G.; Branas, C.C.; Chihuri, S.; Mehranbod, C.; Li, G. The Unknown Denominator Problem in Population Studies of Disease Frequency. *Spatial and Spatio-temporal Epidemiology* **2020**, 100361. https://doi.org/10.1016/j.sste.2020.100361.
31. Yang, S.; et al. Early estimation of the case fatality rate of COVID-19 in mainland China: a data-driven analysis. *Annals of translational medicine* **2020**, 8. https://doi.org/10.21037/atm.2020.02.66.
32. Baud, D.; et al. Real estimates of mortality following COVID-19 infection. *The Lancet infectious diseases* **2020**, 7, 773. https://doi.org/10.1016/S1473-3099(20)30195-X.
33. Pueyo, T. Coronavirus: Why you must act now. Politicians, community leaders and business leaders: what should you do and when? 2020 Mar 10. https://medium.com/@tomaspueyo/coronavirus-act-today-or-people-will-die-f4d3d9cd99ca.
34. Tian, S.; et al. Characteristics of COVID-19 infection in Beijing. *Journal of Infection* **2020**, 80, 401-406. https://doi.org/10.1016/j.jinf.2020.02.018.
35. Li, L.Q.; et al. COVID-19 patients' clinical characteristics, discharge rate, and fatality rate of meta-analysis. *Journal of medical virology* **2020**, 92, 577-583. https://doi.org/10.1002/jmv.25757.
36. Khafaie, M.A.; Rahim, F. Cross-country comparison of case fatality rates of COVID-19/SARS-COV-2. *Osong Public Health and Research Perspectives* **2020**, 11, 74. https://doi.org/10.24171/j.phrp.2020.11.2.03.
37. Bhatraju, P.K.; et al. Covid-19 in critically ill patients in the Seattle region—case series. *New England Journal of Medicine* **2020**, 382, 2012-2022. https://doi.org.10.1056/NEJMoa2004500.

38. Felice, C.; et al. Use of RAAS inhibitors and risk of clinical deterioration in COVID-19: results from an Italian cohort of 133 hypertensives. *American Journal of Hypertension* **2020**. https://doi.org/10.1093/ajh/hpaa096.
39. Souch, J.M.; Cossman, J. S. A Commentary on Rural-Urban Disparities in COVID-19 Testing Rates per 100,000 and Risk Factors. *The Journal of Rural Health* **2020**. https://doi.org/10.1111/jrh.12450.
40. Jefferson T.; Heneghan C. Covid 19—Epidemic 'Waves'. Centre for evidence-based medicine April 30. **2020** https://www.bebm.net/covid-19/covid-19-epidemic-waves/
41. Donell, S.T.; et al. Preparation for the next COVID-19 wave: The European Hip Society and European Knee Associates recommendations. *Knee Surgery, Sports Traumatology, Arthroscopy* **2020**, 1-9. https://doi.org/10.1007/s00167-020-06213-z.
42. Xinhua, 2020-07-07. Over 11 Million in Beijing Given COVID-19 Test, Beijing Fights Against COVID-19. http://english.beijing.gov.cn/specials/COVID19/latest/202007/t20200707_1940942.html.
43. Coccia, M. The impact of first and second wave of the COVID-19 pandemic in society: comparative analysis to support control measures to cope with negative effects of future infectious diseases. *Environmental Research* **2021**, 197, 111099. https://doi.org/10.1016/j.envres.2021.111099.
44. Plackett, R. L. Karl Pearson and the chi-squared test. *International Statistical Review/Revue Internationale de Statistique* **1983**, 59-72. https://doi.org/10.2307/1402731.
45. Gerald, B. A brief review of independent, dependent and one sample t-test. *International Journal of Applied Mathematics and Theoretical Physics* **2018**, *4*, 50-54. https://doi.org/10.11648/j.ijamtp.20180402.13.